Lindemann melting criterion and the Gaussian core model

F. H. Stillinger and T. A. Weber
Bell Laboratories, Murray Hill, New Jersey 07974
(Received 2 May 1980)

A series of molecular-dynamics calculations has been carried out to examine melting in the classical Gaussian core model at reduced density $\rho^* = 0.2$. The stable crystal form at this density is body-centered cubic. Thermal equilibrium values of mean-square particle displacement have been evaluated over the entire temperature range below melting. As a result the Lindemann ratio f (of rms displacement to lattice spacing at the melting point) was found to be 0.160 ± 0.005, considerably larger than Shapiro's estimate for several bcc metals. This finding further undermines the Lindemann hypothesis that f should be constant for all solids of a given crystal structure at their melting points.

I. INTRODUCTION

One of the oldest and simplest criteria for the melting of solids is the Lindemann rule.[1] This rule states that melting occurs when the mean amplitude of thermal motion for a particle in the crystal reaches some characteristic fraction f of the spacing a between nearest neighbors:

$$\langle(\vec{u})^2\rangle^{1/2}/a = f \quad . \tag{1}$$

Here $\vec{u}$ is the displacement measured from the stable lattice position. While the original Lindemann study suggested that f ought to be close to $\frac{1}{2}$, subsequent work seems to reveal that rather smaller values are appropriate, depending in fact upon the crystal structure involved. Using harmonic lattice dynamics, Shapiro[2] has found, for example, that f is close to 0.113 for all five of the bcc alkali metals, while 0.071 is the value appropriate for the fcc metals Al, Cu, Ag, and Au. The latter f value agrees reasonably well with experimental results for Al and Cu determined by Martin and O'Connor[3] by Bragg diffraction of Mössbauer x-rays from an ^{57}Fe source.

As computer simulation of classical many-body systems has become more and more popular it has become feasible to check the quantitative validity of the Lindemann rule for a variety of model interactions. Hansen[4] has studied the case of the Lennard-Jones$^{6-12}$ potential (for which the crystal structure is fcc) and finds that f along the melting line is nearly temperature independent and in the range 0.14 to 0.15, roughly twice the Shapiro value for metals. Young and Alder[5] have carefully investigated the extremely anharmonic rigid-sphere model (also fcc in its crystalline phase) and obtain results showing that f is 0.14. Hoover, Gray, and Johnson[6] have applied both lattice dynamics and Monte Carlo computer simulation to model fcc crystals whose particles interact with simple inverse-power potentials, finding once again that f lies close to 0.15.

Even admitting the possibility of some error in these various results, it appears that the Lindemann hypothesis has been significantly violated for the fcc structure. At this stage it seems worthwhile to examine the parallel case of the bcc structure, for which Shapiro's f value 0.113 stands alone and unchallenged. It is in this spirit that we have investigated the Lindemann rule for the Gaussian core model.

II. GAUSSIAN CORE MODEL

In reduced units that are most natural to the problem, the Gaussian core model has the following simple potential-energy function:

$$\Phi = \sum_{i<j=1}^{N} \exp(-r_{ij}^2) \quad . \tag{2}$$

It is known[7] that the stable crystal form at low density is fcc, while at high density it is bcc. At absolute-zero temperature the respective regions of stability are the following ranges of reduced density:

$$\rho^* < 0.179\,407 \text{ (fcc)} \quad , \quad \rho^* > 0.179\,767 \text{ (bcc)} \quad . \tag{3}$$

In the low-density–low-temperature limit this model is known to reduce to the rigid-sphere model.[7]

Owing to the penetrability, or softness, of its pair potential the Gaussian core model exhibits unusual properties. Molecular-dynamics simulation[8] reveals that at high density ($\rho^* \geq 0.4$) the behavior is distinctly "waterlike," with negative melting volumes,

and with negative thermal expansion and negative temperature coefficient of self-diffusion in the fluid phase. Furthermore, it has been established[7,8] that the melting temperature of the bcc phase goes to zero as its density increases to infinity. Because these anomalies are not shared by any of the other real substances or theoretical models for which the Lindemann rule has been tested, it seems especially worthwhile expending some effort to see how the Gaussian core model compares with prior results.

In order to place the Gaussian core model in context, it is useful to interpret the Gaussian potential at a given distance r in terms of an effective inverse-power potential. By matching logarithmic derivatives for the two functions one finds that the exponent of the inverse-power form must be[7]

$$n^*(r) = 2r^2 \quad . \tag{4}$$

By inserting the nearest-neighbor distance for the bcc crystal at density ρ^*,

$$n^*(a) = 6(4\rho^*)^{2/3} \quad . \tag{5}$$

This is 6.96 at $\rho^* = 0.2$, the density of primary interest in the present paper, and indicates a rather softer replusive core than usually assumed for realistic pair potentials.

The core softness exhibited by the Gaussian potential suggests that in a crude way this model might be useful for studying matter under extreme compression, where electron valence shells have begun to break down to produce conduction electrons. With this as its motivation, an Appendix shows how a rough correspondence can be established between thermodynamic states of the Gaussian core model and those of the real monatomic substance Ar. With this correspondence the $\rho^* = 0.2$ density of the former is equivalent to the latter at about 5 times its triple-point liquid density, and the implied pressure in the Ar is about 5.5 megabars.

III. MOLECULAR DYNAMICS TECHNIQUE

Our previous molecular-dynamics work on the Gaussian core model[8,9] examined properties at the two densities $\rho^* = 0.4, 1.0$. In the present project we have focused entirely on the lower density $\rho^* = 0.2$. As before, the stable solid phase at low temperature is bcc.

To initiate the computations $N = 432$ particles were placed within a unit cube of the proper size for the given density. The starting positions corresponded to a perfect bcc arrangement. Periodic boundary conditions were imposed. Interactions were disregarded during the computation for all pairs of particles sufficiently far apart that the Gaussian function satisfied the inequality

$$\exp(-r^2) < \exp(-28) \approx 7 \times 10^{-13} \quad . \tag{6}$$

Initial momenta were assigned by a random-number generator, and corresponded to a temperature very much lower than the melting temperature. Subsequent changes in temperature were effected by rescaling momenta at the end of a previously completed run, followed by a relaxation run to achieve equilibration in the new state.

The differential equations of motion were integrated using Gear's fifth-order algorithm[10] and a step size in reduced units (particle mass = 1)

$$\Delta t^* = 0.05 \quad . \tag{7}$$

Average values were computed for each state during runs of 4000 steps (following relaxation runs) during which total energy and total momentum remained virtually unchanged.

Melting and freezing in these calculations are monitored by a wide variety of properties, including pressure, mean potential energy, pair-correlation function, and self-diffusion constant. Changes of phase are unambiguous and create striking changes in all of the cited properties. Hysteresis is invariably observed; the solid superheats and the fluid undercools. Figure 1 shows this hysteresis for the mean interaction energy per particle, $\langle \Phi \rangle / N$, giving curves that are a summary of many separate determinations. We presume that the position of the thermodynamic melting point T_m^* falls close to the center of the hysteresis loop,[8] and on that basis we believe

$$T_m^* \approx 8.12 \times 10^{-3} \quad (\rho^* = 0.2) \quad . \tag{8}$$

The melting entropy is estimated to be

$$\Delta S / N k_B \approx 0.847 \quad (\rho^* = 0.2) \quad . \tag{9}$$

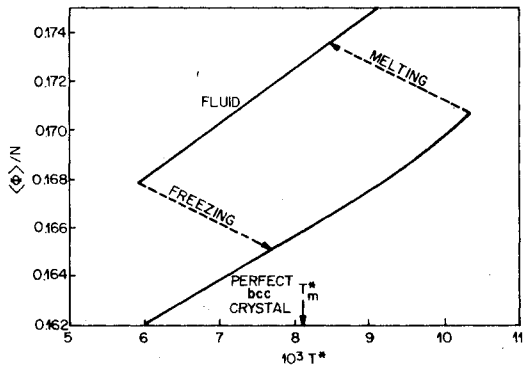

FIG. 1. Mean interaction energy for the Gaussian core model at $\rho^* = 0.2$.

Figure 2 shows the time dependence of

$$A(t^*) = N^{-1} \sum_{j=1}^{N} [\vec{r}_j(t^*) - \vec{r}_j(0)]^2 \tag{10}$$

for a single molecular-dynamics run carried out on the perfect bcc crystal at a temperature somewhat below T_m^*. Its form is typical. Notice that an average *only* over particles is involved, *not* over time. In spite of the natural fluctuations present it is obvious that a plateau region is achieved well before the end of the run (at $t^* = 200$). We subsequently calculate the time-averaged mean-square displacement $\langle(\Delta\vec{r})^2\rangle$ by averaging $A(t)$ over the last half of the dynamical run:

$$\langle(\Delta\vec{r})^2\rangle = \frac{1}{100}\int_{100}^{200} A(t^*)dt^* \ . \tag{11}$$

In principle, self-diffusion ought to be present in the solid at any temperature above absolute zero. Its presence would cause $A(t^*)$ to display a linear upward drift with time from whose slope the self-diffusion constant could be inferred. In practice we find that solid-state diffusion is not perceptibly present at or below T_m^*. The number of particles employed in this study, 432, has just the right form as an integer ($N = 2n^3$) to permit a defect-free crystal to exist in the system, aligned with the principal directions of the unit cell, and fitting perfectly to the image systems at all six cell faces. Spontaneous creation of point defects that would assist diffusion (interstitials and vacancies) is apparently very improbable below T_m^* for the system size considered. Of course the diffusion process could artifically be encouraged by changing N slightly from 432.

As the crystal is heated beyond T_m^* it becomes increasingly unstable and shakes apart quickly at an effective superheating limit around $T^* = 10^{-2}$. Upon approaching this point by slow superheating, defects can be spontaneously formed and diffusion becomes observable.

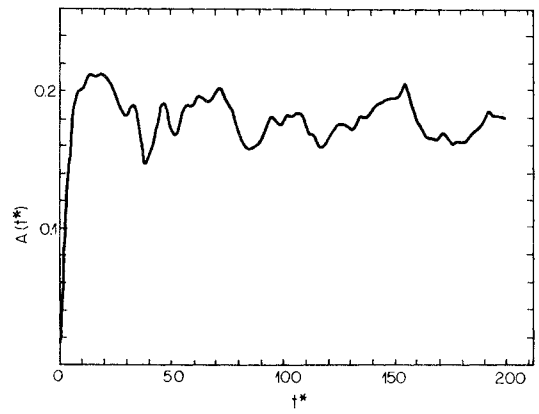

FIG. 2. Squared displacement vs time, averaged over particles, for a molecular-dynamics run at $T^* = 7.899 \times 10^{-3}$, $\rho^* = 0.2$.

IV. RESULTS

Figure 3 shows our calculated $\langle(\Delta\vec{r})^2\rangle$ values. Points are plotted for 35 distinct molecular-dynamics runs, generated both during heating and cooling portions of the overall sequence. Although some scatter is obviously present we believe that the points shown genuinely reflect the correct behavior of the Gaussian core model at this density.

The upward curvature displayed by results in Fig. 3 is due to anharmonicity. At the melting temperature T_m^* we estimate that this anharmonicity causes $\langle(\Delta\vec{r})^2\rangle$ to be about 10% above the linear extrapolation of low-temperature harmonic results. Similarly we find that the increment in mean potential energy $\langle\Phi\rangle/N$ over its value at absolute zero is about 9% larger at T_m^* than harmonic motion alone would produce.

Because the positions of any given particle at widely separated times are uncorrelated, we have

$$\langle(\Delta\vec{r})^2\rangle = 2\langle(\vec{u})^2\rangle \ . \tag{12}$$

This permits the Lindemann ratios, Eq. (1), to be inferred. The right-hand vertical scale in Fig. 3 shows

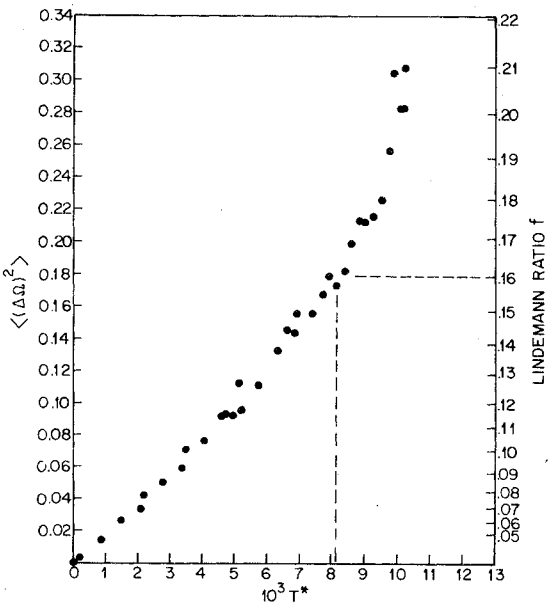

FIG. 3. Mean-square particle displacements vs temperature and the associated Lindemann ratios. Gaussian core model at $\rho^* = 0.2$ in the defect-free bcc crystal. The thermodynamic melting point is indicated by dashed lines.

these f values. From the figure one sees that

$$f(T_m^*) = 0.160 \pm 0.005 \ , \tag{13}$$

a value substantially in excess of Shapiro's result for the bcc alkali metals, 0.113. The Gaussian core model exhibits the latter f value at $T^* \approx 4.7 \times 10^{-3}$, which is sufficiently far below our presumed T_m^* that the discrepancy can hardly arise from an error in identifying this melting temperature.

V. DISCUSSION

The clear implication of the results shown in Eq. (13) is that the Lindemann rule is susceptible to significant violation for bcc as well as fcc solids. It seems likely that f will be found to be potential dependent for any given crystal structure.

Because the properties of the Gaussian core model become increasingly anomalous as density increases it is desirable to redetermine f for $\rho^* > 0.2$. A naive guess would be that the resulting f's would be even larger and would constitute an even more drastic violation of the Lindemann rule. Unfortunately it is more difficult to induce spontaneous freezing in the model at these elevated densities, which implies some extra uncertainty in locating T_m^*. In any case mapping out a curve such as that shown in Fig. 3 is a major computational undertaking.

Hoover, Gray, and Johnson[6] have claimed that estimates of f using small-system calculations lie below the proper f value for the infinite system limit. Specifically they suggest that the negative error is proportional to $N^{-1/3}$, where N is the number of particles used in the calculation. Although we have not checked this matter in our own study, it is worth stressing that if such a correction were to be applied to Eq. (13) the discrepancy with Shapiro's result[2] would only widen.

In a recent study of crystal nucleation from the melt, Hsu and Rahman[11] have shown by molecular-dynamics simulation that a pair potential constructed to describe Rb (one of the metals considered by Shapiro) leads to a stable bcc crystal. This potential has an infinite number of maxima and minima (reflecting the contribution of a Fermi sea of conduction electrons). In view of the paucity of direct determinations of f for bcc crystals, either experimental or theoretical, it would be enlightening to perform the requisite molecular-dynamics determination of f for a perfect bcc crystal with this interaction.

Finally, we remark that we have examined $\langle(\Delta\vec{r})^2\rangle$ for defective crystals (both bcc and fcc) in the Gaussian core model at $\rho^* = 0.2$. These have been generated by spontaneous nucleation of the supercooled fluid. On account of the random nature of nucleation, crystals formed in this manner are usually misaligned with respect to the sides of the unit cube employed in the calculation. When they grow to encounter their periodic images, mismatch at the seam arises. The end product is strained, and contains both point defects and extended defects. We have typically found that the $\langle(\Delta\vec{r})^2\rangle$ values for any such sample vs T^* describes a curve that lies *above* the one shown in Fig. 3 for the perfect bcc crystal. Enhancements of 30% were frequently observed. Unfortunately it is difficult to assign a precise melting temperature to any one such defective sample.

APPENDIX

The Lennard-Jones (LJ) 6-12 potential

$$V_{\rm LJ}(R) = \epsilon\phi_{\rm LJ}(R/\sigma) \ , \quad \phi_{\rm LJ}(x) = 4(x^{-12} - x^{-6}) \ , \tag{A1}$$

can adequately represent the interactions in Ar with the following choice of parameters[12]:

$$\begin{aligned} &\sigma = 3.44 \text{ Å} \ , \\ &\epsilon = 120 \text{ K} \times k_B \\ &\quad = 1.6565 \times 10^{-14} \end{aligned} \tag{A2}$$

in units of erg/atom.

In order to establish contact with the Gaussian core model we first construct a fit to $\phi_{\rm LJ}$ near its minimum using a linear combination of *two* Gaussians:

$$\phi_{2G}(x) = A \exp(-\alpha x^2) - B \exp(-\beta x^2) \ . \tag{A3}$$

The four constants A, α, B, and β are fixed by requiring ϕ_{2G} to mimic $\phi_{\rm LJ}$ in the following four respects:

$$\phi_{2G}(1) = \phi_{\rm LJ}(1) = 0 \ ; \tag{A4}$$

$$\phi_{2G}(2^{1/6}) = \phi_{\rm LJ}(2^{1/6}) = -1 \ ; \tag{A5}$$

$$\phi'_{2G}(2^{1/6}) = \phi'_{\rm LJ}(2^{1/6}) = 0 \ ; \tag{A6}$$

$$\phi''_{2G}(2^{1/6}) = \phi''_{\rm LJ}(2^{1/6}) = 72/2^{1/3} \ . \tag{A7}$$

These simultaneous equations can be solved numerically to yield

$$\begin{aligned} &A = 7\,073.856\,194, \quad \alpha = 8.332\,099\,803 \ , \\ &B = 6.639\,106\,684, \quad \beta = 1.360\,916\,181 \ . \end{aligned} \tag{A8}$$

Figure 4 shows a plot of ϕ_{2G} and of the difference $\Delta\phi = \phi_{\rm LJ} - \phi_{2G}$. The fit is indeed close over most of the attractive well. Naturally ϕ_{2G} fails to display the proper long-range tail of $\phi_{\rm LJ}$, but in the region where the discrepancy is the largest ($x \approx 1.88$) both functions are small. In the "core region," $x < 1$, ϕ_{2G}

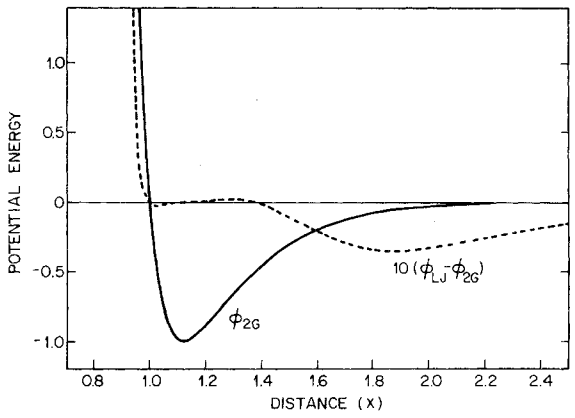

FIG. 4. Two Gaussian approximation to the Lennard-Jones potential.

rises less rapidly than ϕ_{LJ}. It should be noted that experimental studies of this core region for pairs of real atoms colliding at high energy generally reveal that ϕ_{LJ} has too impenetrable a core.[13]

Under the circumstances it is not implausible to use ϕ_{2G} to represent interactions in Ar under conditions of very high pressure and/or temperature. But under such conditions the structure and properties of the substance would be dominated by the first term in ϕ_{2G}; the second negative term would be negligible. Thus interactions in Ar would effectively have been reduced to single repelling Gaussians acting between each pair of particles, in other words, the Gaussian core model examined in the body of this paper.

Conversion is now straightforward between reduced variables (with asterisks) used in the Gaussian core calculations and variables (no asterisks) used to describe the corresponding state of Ar. Number density, temperature, and pressure transform in the following way:

$$\rho = \alpha^{3/2}\sigma^{-3}\rho^* = 0.5908\rho^* \quad \text{(A9)}$$

expressed in atoms/Å^3;

$$T = (\epsilon A/k_B)T^* = 8.4886\times 10^5 T^* \quad \text{(A10)}$$

in K;

$$p = \epsilon A\,\alpha^{3/2}\sigma^{-3}p^* = 6.923\times 10^7 p^* \quad \text{(A11)}$$

in bars.

At the reduced density $\rho^* = 0.2$ investigated in this paper, the number density of Ar implied by Eq. (A9) is 0.1182 atoms/Å^3. This may be compared with the value 0.02130 atoms/Å^3 for liquid Ar at its normal freezing point (84 K).[14] Equation (A10) converts the melting temperature T_m^*, Eq. (8), to

$$T = 6893 \quad \text{(A12)}$$

in K. The fluid-phase pressure p^* at this transition point is found to be 7.975×10^{-2}, so Eq. (A11) implies (in bars).

$$p = 5.521\times 10^6 \ . \quad \text{(A13)}$$

Finally, we can relate the dimensionless time t^* in the Gaussian core calculations to real time t for Ar:

$$t = \sigma(m/\alpha A\,\epsilon)^{1/2}t^* = 8.9666\times 10^{-15}t^* \quad \text{(A14)}$$

expressed in sec. Here $m = 6.6336\times 10^{-23}$ g is the mass of an Ar atom. From this last result we see that each 4000-step molecular-dynamics run ($t^* = 200$) amounts to an elapsed time of 1.7933 psec.

[1]F. A. Lindemann, Phys. Z. 11, 609 (1910).
[2]J. N. Shapiro, Phys. Rev. B 1, 3982 (1970).
[3]C. J. Martin and D. J. O'Connor, J. Phys. C 10, 3521 (1977).
[4]J.-P. Hansen, Phys. Rev. A 2, 221 (1970).
[5]D. A. Young and B. J. Alder, J. Chem. Phys. 60, 1254 (1974).
[6]W. G. Hoover, S. G. Gray, and K. W. Johnson, J. Chem. Phys. 55, 1128 (1971).
[7]F. H. Stillinger, J. Chem. Phys. 65, 3968 (1976).
[8]F. H. Stillinger and T. A. Weber, J. Chem. Phys. 68, 3837 (1978).
[9]F. H. Stillinger and T. A. Weber, J. Chem. Phys. 70, 4879 (1979).
[10]C. W. Gear, Argonne National Laboratory Report No. ANL-7126, January, 1966 (unpublished).
[11]C. S. Hsu and A. Rahman, J. Chem. Phys. 71, 4974 (1979).
[12]J. O. Hirschfelder, C. F. Curtiss, and R. B. Bird, *Molecular Theory of Gases and Liquids* (Wiley, New York, 1954), p. 1110.
[13]R. B. Bernstein and J. T. Muckerman, in *Advances in Chemical Physics*, edited by J. O. Hirschfelder (Wiley-Interscience, New York, 1967), Vol. 12, pp. 392, 393.
[14]R. J. Meyer, *Gmelins Handbuch der Anorganischen Chemie. Edelgase* (Verlag Chemie G.M.B.H., Leipzig, 1926), p. 139.